

Analysis of thermal fatigue behaviour of brittle structural materials

J. P. SINGH, K. NIIHARA, D. P. H. HASSELMAN

Department of Materials Engineering, Virginia Polytechnic Institute and State University, Blacksburg, Virginia 24061, USA

The effect of the level of maximum temperature (T_{\max}), the temperature range (ΔT) and the mode of convective heat transfer on the thermal fatigue resistance of brittle structural materials is analysed. Expressions are derived for the number of thermal cycles to failure in terms of the appropriate mechanical and thermal properties, crack growth parameter, ΔT and T_{\max} . For simultaneous changes in T_{\max} and ΔT commonly used in practice, the change in thermal fatigue life is governed by both the thermal stress intensity exponent (n) and the activation energy (Q) for subcritical crack growth, in contrast to the results of other studies. For constant T_{\max} but variable ΔT , thermal fatigue life is affected by n only, whereas, for constant ΔT but variable T_{\max} , the value of Q alone governs changes in fatigue-life. Heat transfer by natural or forced convection will result in differences in thermal fatigue resistance. Recommendations are made for the design and analysis of thermal fatigue experiments. Figures-of-merit for the selection of materials with high thermal fatigue resistance are presented.

1. Introduction

Brittle structural materials can exhibit static [1, 2], dynamic [3, 4] and cyclic [5, 6], as well as thermal [7, 8], fatigue. These mechanisms of fatigue result from sub-critical crack growth due to stress-corrosion at low temperatures or diffusional mechanisms at high temperatures. For the purpose of reliable design of structures or components made of brittle materials, it is imperative that the mechanisms responsible for fatigue are qualitatively, as well as quantitatively, well understood. An extensive literature indicates that the "failure-prediction" of brittle materials subjected to static [9, 10], dynamic or cyclic fatigue [11] under isothermal conditions appears well-understood. The statistical nature of brittle fracture can also be incorporated into predictions of fatigue-behaviour.

The thermal fatigue behaviour of brittle materials is more complex for the principal reasons that both the stresses and temperatures change simultaneously, requiring numerical techniques for the calculations of thermal fatigue behaviour. In a number of such studies [12-14], reasonable to excellent agreement was found between laboratory

data and the predicted number of thermal cycles-to-failure. More recently, by analysing experimental data for thermal fatigue behaviour of a number of brittle structural materials, Kamiya and Kamigaito [15] obtained quantitative information on the behaviour of sub-critical crack growth during thermal fatigue.

In order to provide a basis for the objectives of the present study, it should be noted that for convective heat transfer used in most thermal fatigue studies the magnitude of the transient thermal stresses is a function of the temperature differences encountered. The rate of sub-critical crack growth, however, is a function of the thermal stresses as well as the absolute temperatures involved. These two separate effects are critical to the design of a thermal fatigue experiment as well as to the analysis of the data obtained.

In general, the thermal fatigue behaviour of a material is established by measuring the number of thermal cycles (N) required to cause failure of appropriate specimens cycled over a temperature range, ΔT , between an upper temperature, T_{\max} , and a lower temperature, T_{\min} . Fig. 1 schematically

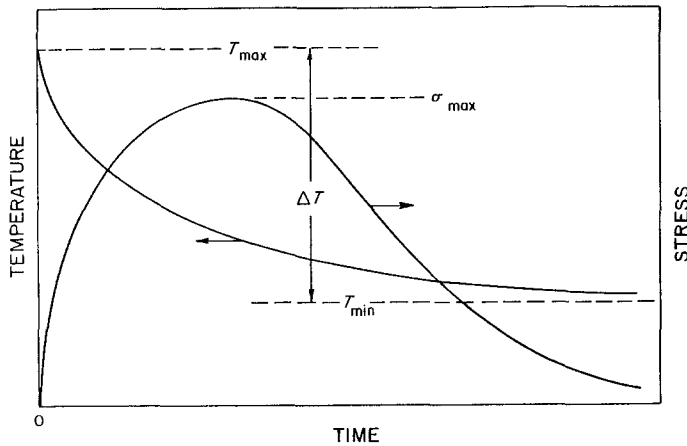


Figure 1 Schematic representation of the time-dependence of the temperature and stress in the surface of a thermal fatigue specimen.

shows the time-dependence of the temperatures and stresses in the surface of a thermal fatigue specimen.

A complete thermal fatigue curve is established by determining the number of thermal cycles N for a range of values of ΔT . However, critical to the results obtained is the specific way in which ΔT is varied. Commonly, ΔT is varied by lowering the upper temperature, T_{\max} , while the lower temperature, T_{\min} , is kept constant. In this case the magnitude of the stresses as well as the absolute values of temperature are varied. If ΔT were changed by raising (or lowering) T_{\min} , the stresses are varied, but the absolute temperatures at which most of the crack growth takes place are kept constant. Similarly, ΔT can be kept constant, by changing T_{\max} and T_{\min} by an equal amount. Depending on the kinetics of crack growth, these three different conditions are expected to lead to differences in thermal fatigue behaviour as measured by the number of cycles-to-failure. A further complexity is introduced by noting that heat transfer can occur in a forced or natural convective mode. In forced convection, heat transfer is Newtonian, i.e. the heat transfer coefficient is independent of the difference in instantaneous temperature of the surface of the specimen and the temperature of the fluid medium used for heating or cooling the specimen. In contrast, for natural convection, the heat transfer coefficient is a non-linear function of the difference in instantaneous surface temperature and the temperature of the fluid medium [16]. Under these conditions the heat transfer coefficient changes as the specimen changes in temperature (see Fig. 1) towards thermal equilibrium. Detailed calculation of this effect by the finite element method, to be

reported elsewhere [17], showed that for a given material and specimen size and identical values of the heat transfer coefficient at the beginning of the thermal cycle, the magnitude of the maximum thermal stress under conditions of natural convection, are significantly less than the corresponding values for forced convection.

It is the purpose of this study to present an analytical treatment of the temperature and heat transfer variables in the thermal fatigue resistance of brittle materials, in order to establish guidelines for the design of thermal fatigue experiments and analysis of the data in terms of crack-growth behaviour.

2. Analysis

2.1. General

The analysis will concentrate on thermal fatigue specimens in the shape of long cylinders with circular cross-section. For this geometry, solutions for the thermal stresses are available [17, 18]. The ends of the specimens are assumed to be thermally insulated so that fracture at the ends is avoided. This assumption will permit the use of the thermal stresses calculated for circular cylinders of infinite length. It is further assumed that the thermal fatigue mechanism operates only during the cooling part of the cycle. This latter assumption is reasonable since under those conditions the stresses exceed those during heating and are a maximum in the specimen surface most susceptible to stress-corrosion and the introduction of flaws during specimen preparation and handling. The results of the analysis can be easily extended to other specimen geometries or thermal fatigue during heating or combinations of heating and cooling. Finally it is assumed that between thermal

cycles the specimen comes to thermal equilibrium so that overlapping of the transient thermal stresses of successive thermal cycles need not be considered.

2.2. Theory

The rate of sub-critical crack growth (\dot{a}) under conditions of thermal fatigue will be assumed to be identical to the expression for isothermal conditions given by

$$\dot{a} = AK_I^n \exp(-Q/RT), \quad (1)$$

where A is a constant, n is the stress intensity exponent, K_I is the Mode I stress-intensity factor, Q is the activation energy, R is the gas constant and T is the absolute temperature.

In terms of the thermal stress (σ) and crack size (a), K_I is defined by

$$K_I = Y\sigma a^{1/2}, \quad (2)$$

where Y is a constant related to the stress distribution and the geometry of the crack. Implicit in the use of Equation 2, is the assumption that, over the total range of crack growth, the crack size remains sufficiently small, compared to the size of the specimen, that the compliance of the specimens remains unaffected. This will permit calculation based on thermo-elastic theory. In this manner, the complexity of the effect of the presence of the crack on the thermal stress field and thermal stress intensity factor, which would require numerical methods, is avoided.

For a given value of thermal stress, failure will occur at a critical crack size, a_c such that $K_I = K_{Ic}$, the critical stress intensity factor. The thermal fatigue life is defined by the number of thermal cycles required to propagate the crack from an initial crack size, a_0 to the critical crack size, a_c .

In direct analogy to the time-to-failure under isothermal conditions, the number of cycles-to-failure (N) in thermal fatigue can be expressed

$$N = B \int_0^{K_{Ic}} \frac{K_I dK_I}{\dot{a}\sigma^2(t) Y^2}, \quad (3)$$

where B is a constant and $\sigma(t)$ is the transient thermal stress. Because of the relative complexity of the analytical expressions for the transient temperatures and stresses even for the simple geometry such as a solid circular cylinder, the integration of Equation 3 is most conveniently carried out by numerical methods, such as those employed in a number of previous investigations [12, 19, 20].

However, in order to obtain a convenient analytical expression for the number of cycles-to-failure, a number of simplifying, but entirely reasonable assumptions are made. Firstly, as indicated by Fig. 1, any temperature during the thermal cycle can be expressed as a fractional value of the maximum temperature, T_{\max} , at the beginning of the thermal cycle. For this reason, the effect of the thermally activated nature of the crack growth on thermal fatigue life can be expressed uniquely in terms of a factor $\exp(Q/RT_{\max})$. Secondly and similarly, any value of the transient thermal stress during the thermal cycle can be expressed as a function of the maximum value of thermal stress, σ_{\max} encountered during the thermal cycle. Furthermore, the analytical results for the time-to-failure [10] under isothermal, constant stress conditions, indicate that unless the total extent of crack growth is small, the time-to-failure is an inverse function of the value of the stress intensity factor at the time ($t = 0$) of the application of the load. For these latter two reasons, it will be assumed that the number of cycles-to-failure, as affected by the stress-intensity factor, can be uniquely defined in terms of an inverse function of the maximum value of the thermal stress intensity factor (K_{Ii}) encountered during the first thermal cycle. In effect this changes the lower limit of the integral of Equation 3 from zero to K_{Ii} . Furthermore, it will be assumed that the number of thermal cycles-to-failure is an inverse function of the time-duration over which the transient thermal stress acts for each cycle. Analytical results [18] for the thermal stresses indicate that the magnitude of stress as a function of time can be expressed in terms of a non-dimensional time, $\tau = \kappa t/R^2$, where κ is the thermal diffusivity, t is the real time and R is the radius of the cylinder. For any material and specimen size, the time period of each thermal stress pulse is proportional to R^2/κ making the number of cycles-to-failure proportional to κ/R^2 .

Substitution of Equation 1 into Equation 3 and incorporation of the above conclusions, the number of thermal cycles-to-failure, in analogy to the time-to-failure under isostress and isothermal conditions, can be written in the general form

$$N = \frac{C\kappa \exp(Q/RT_{\max})}{A\sigma_{\max}^2 R^2 Y^2 (n-2) K_{Ii}^{(n-2)}}, \quad (4)$$

where C is a constant which, in principle, can be obtained by numerical integration of Equation 3

and K_{II} is defined by

$$K_{II} = Y\sigma_{\max}a_1^{1/2}. \quad (5)$$

Substitution of Equation 5 into Equation 4, results in the value of N expressed directly in terms of the maximum value of the thermal stress

$$N = \frac{Ck \exp(Q/RT_{\max})}{R^2 \sigma_{\max}^n A(n-2) Y^n a_1^{(n-2)/2}}. \quad (6)$$

2.3. Derivation of thermal fatigue-life

2.3.1. Forced convection

Under forced convection, the heat transfer coefficient is independent of the range of temperature difference over which the specimen is being cycled. Over the range of the Biot number, $1 < \beta < 20$, the maximum value of tensile thermal stress in the surface of a circular rod can be expressed to a very good approximation by [18, 21]

$$\sigma_{\max}^{-1} = \frac{(1-\nu)}{\alpha E \Delta T} (1.45 + 4.95/\beta), \quad (7)$$

where α is the coefficient of thermal expansion, E is Young's modulus of elasticity, ν is Poisson's ratio, ΔT is the temperature range over which the specimen is being cycled ($\Delta T = T_{\max} - T_{\min}$, see Fig. 1) and $\beta = Rh/k$ where R is the cylinder radius, h is the heat transfer coefficient and k is the thermal conductivity.

Substitution of Equation 7 into Equation 6 yields

$$N = \frac{Ck}{Y^n (n-2) AR^2 a_1^{(n-2)/2}} \times \left(\frac{1-\nu}{\alpha E \Delta T} \right)^n (1.45 + 4.95/\beta)^n \exp(Q/RT_{\max}). \quad (8)$$

In order to establish the nature (slope, etc) of a thermal fatigue curve for a given material it is most convenient to derive expressions for the ratio of the values of N for two conditions of thermal fatigue. As discussed earlier, there are three basic ways in which a thermal fatigue experiment can be carried out: (1) ΔT can be varied by raising or lowering T_{\max} , keeping T_{\min} constant; (2) ΔT can be varied by keeping T_{\max} constant and raising or lowering T_{\min} and (3) ΔT can be kept constant by raising or lowering T_{\max} and T_{\min} by equal amounts.

The effect of these three changes in temperature on thermal fatigue-life will be different.

For analytical purposes, it is most convenient

to examine these quantitatively by deriving expressions for the ratio of the number of cycles-to-failure for small differences in T_{\max} , T_{\min} or ΔT , which yield the following results.

2.3.1.1. ΔT varied; T_{\max} constant. For this condition, the ratio of the number of cycles-to-failure N_1 and N_2 for values of ΔT_1 and ΔT_2 , respectively, is

$$N_1/N_2 = (\Delta T_1/\Delta T_2)^{-n}. \quad (9)$$

2.3.1.2. ΔT constant; T_{\max} varied. For two values of $T_{1,\max}$ and $T_{2,\max}$ the ratio of the number of cycles-to-failure N_1 and N_2 , respectively, is

$$N_1/N_2 = \exp \left[\frac{Q}{R} \left(\frac{1}{T_{1,\max}} - \frac{1}{T_{2,\max}} \right) \right]. \quad (10)$$

2.3.1.3. ΔT varied; T_{\min} constant. For this condition the ratio of the number of cycles-to-failure N_1 and N_2 for values of ΔT_1 and ΔT_2 , respectively, becomes

$$\frac{N_1}{N_2} = \left(\frac{\Delta T_1}{\Delta T_2} \right)^{-n} \exp \left[\frac{Q}{R} \left(\frac{1}{T_{1,\max}} - \frac{1}{T_{2,\max}} \right) \right]. \quad (11)$$

2.3.2. Natural convection

Under conditions of natural convection the heat transfer coefficient is a function of the instantaneous temperature difference (ΔT_i) between the specimen surface and the fluid medium. For values of the Grashof, Prandtl and Nusselt numbers appropriate for laboratory studies of thermal fatigue behaviour, the heat transfer coefficient, h , can be expressed [16] as

$$h = C'(\Delta T_i)^{1/4}, \quad (12)$$

where C' is a constant which depends on the properties of the fluid medium such as the viscosity, density, thermal expansion, specific heat and thermal conductivity as well as on the size of the structure being heated or cooled. Equation 12 indicates that the heat transfer coefficient decreases as the difference in temperature between the specimen surface and medium (ΔT_i) decreases during the transient heat transfer. In accepting the validity of Equation 12, it is implicitly assumed that during the transient heat transfer, conditions for natural free convection pertain, which essentially is a steady-state phenomenon.

The transient thermal stresses in a solid cylinder

under natural heat transfer conditions described by Equation 12 were calculated by finite element methods to be reported in detail elsewhere. It was found that the maximum value of the tensile thermal stresses in the surface of the cylinder over the range $0.5 < \beta < 20$, to an excellent approximation, can be written [17].

$$\sigma_{\max}^{-1} = \frac{1-\nu}{\alpha E \Delta T} (1.90 + 6.0/\beta), \quad (13)$$

where the Biot number, β , is now defined in terms of the maximum value of the heat transfer coefficient encountered, i.e. at the value of ΔT_1 in Equation 12 equal to ΔT of the thermal fatigue environment, such that

$$\beta = RC'(\Delta T)^{1/4}/k. \quad (14)$$

With β defined in this manner, a direct comparison of Equations 7 and 13 shows that for the same Biot number the magnitude of maximum thermal stress in natural convection is considerably less than the corresponding value for forced convection.

Substitution of Equation 13 into Equation 6 results in the number of thermal cycles-to-failure under conditions of natural convection

$$N = \frac{Ck}{Y^2(n-2)AR^2a_1^{(n-2)/2}} \times \left(\frac{1-\nu}{\alpha E \Delta T} \right)^n \left[1.9 + \frac{6.0k}{RC'(\Delta T)^{1/4}} \right]^n \exp(Q/RT_{\max}). \quad (15)$$

In direct analogy to the expressions derived earlier in case of forced convection for the ratio of the thermal cycles to failure, corresponding equations for condition of natural convection can also be derived as follows:

2.3.2.1. ΔT varied; T_{\max} constant. From Equation 15, the ratio of the thermal cycles-to-failure N_1 and N_2 , corresponding to values of ΔT_1 and ΔT_2 becomes:

$$\frac{N_1}{N_2} = \left(\frac{\Delta T_1}{\Delta T_2} \right)^{-n} \times \left[1.90 + \frac{6.0k}{RC'(\Delta T_1)^{1/4}} \right]^n \left[1.90 + \frac{6.0k}{RC'(\Delta T_2)^{1/4}} \right]^{-n}. \quad (16)$$

Equation 16 can be presented in simplified

form for the two limiting values of the Biot number

$$\frac{N_1}{N_2} = \left(\frac{\Delta T_1}{\Delta T_2} \right)^{-n} \quad \beta \gg 1 \quad (17a)$$

and

$$\frac{N_1}{N_2} = \left(\frac{\Delta T_1}{\Delta T_2} \right)^{-5n/4} \quad \beta \ll 1 \quad (17b)$$

2.3.2.2. ΔT constant; T_{\max} varied. For two values of $T_{1, \max}$ and $T_{2, \max}$ the ratio of the thermal cycles-to-failure, N_1 and N_2 , respectively, with the aid of Equation 15 can be derived to be

$$\frac{N_1}{N_2} = \exp \left[\frac{Q}{R} \left(\frac{1}{T_{1, \max}} - \frac{1}{T_{2, \max}} \right) \right]. \quad (18)$$

2.3.2.3. ΔT varied, T_{\min} constant. For convenience, the ratio of the thermal cycles-to-failure N_1 and N_2 corresponding to values of ΔT_1 and ΔT_2 and values of $T_{1, \max}$ and $T_{2, \max}$ will be written directly for the high ($\beta \gg 1$) and low ($\beta \ll 1$) Biot number approximations

$$\frac{N_1}{N_2} = \left(\frac{\Delta T_1}{\Delta T_2} \right)^{-n} \exp \left[\frac{Q}{R} \left(\frac{1}{T_{1, \max}} - \frac{1}{T_{2, \max}} \right) \right] \quad \beta \gg 1 \quad (19a)$$

and

$$\frac{N_1}{N_2} = \left(\frac{\Delta T_1}{\Delta T_2} \right)^{-5/4n} \exp \left[\frac{Q}{R} \left(\frac{1}{T_{1, \max}} - \frac{1}{T_{2, \max}} \right) \right] \quad \beta \ll 1. \quad (19b)$$

3. Discussion

The analytical results indicate that the role of the individual parameters specifically n and Q , which affect the kinetics of thermal fatigue crack growth, depends on the method by which a thermal fatigue curve is established. For simplicity, relative thermal fatigue-life will be considered only, such that the discussion can focus in detail on the crack growth variables which affect the ratios of cycles-to-failure for a given thermal environment, material, specimen and crack geometry.

As indicated by Equations 9 and 17, if thermal fatigue life is established by keeping T_{\max} constant and varying ΔT by varying T_{\min} , relative changes in thermal fatigue life are governed only by the stress intensity factor exponent, n . In contrast, as indicated by Equations 10 and 18, if a

thermal fatigue curve is established by keeping ΔT constant and varying T_{\max} and T_{\min} by equal amounts, changes in thermal fatigue life are influenced only by the activation energy for sub-critical crack growth.

If, however, as is common in practice, thermal fatigue behaviour is measured by keeping T_{\min} constant and varying T_{\max} and ΔT by the same amount, changes in thermal fatigue life as indicated by Equations 11 and 19, are affected by both the stress intensity exponent as well as the activation energy for crack growth. Comparing the analytical results for forced and natural convection shows that for the latter (with $\beta \ll 1$) the role of the stress intensity factor exponent (n) is greater than in the former. In the high Biot number approximation, the role of n is identical for both forced and natural convection.

The above conclusions are critical to the design of thermal fatigue experiments and the analysis of experimental data obtained. One significant conclusion is that thermal fatigue data obtained by varying ΔT and T_{\max} simultaneously (which is the usual case) cannot be used to obtain a quantitative value for the stress intensity exponent, by obtaining the value of the slope of $\log N$ against $\log \Delta T$. This latter conclusion is at variance with the recent results of Kamiya and Kamigaito [15], which could lead to misleading results unless due care is exercised.

For the purposes of illustration, a numerical example will be considered on thermal fatigue for hot-pressed polycrystalline silicon nitride subjected to forced convection heat transfer by Ammann *et al.* [13] by cycling appropriate specimens at an initial temperature of near 1600 K into a fluidized bed at approximately 313 K. Appropriate values for the stress intensity exponent and activation energy for sub-critical crack growth are $n \approx 6$ and $Q \approx 170 \text{ kcal mol}^{-1}$, respectively. The change in thermal fatigue life caused by a simultaneous decrease in T_{\max} and ΔT of 20°C will be considered. Substitution of the above values of n and Q into Equation 11 yields the result that due to the decrease in magnitude of thermal stress (i.e. ΔT) thermal fatigue life is increased by 15% (i.e. by a factor of 1.15). In contrast, the decrease in the value of T_{\max} increases thermal fatigue life by a factor equal to 1.97, for a total increase in fatigue life due to both effects equal to 2.26. These numerical results indicate that in silicon nitride the activation energy for slow crack growth

plays a far more important role in establishing thermal fatigue behaviour than the stress intensity exponent. For this reason, a plot of $\log N$ against $\log \Delta T$ of the data of Ammann *et al.* [13] cannot yield a reliable value of n in contrast with the findings of Kamiya and Kamigaito [15]. Because of the relatively small effect of the value of n on thermal fatigue life, it is more appropriate to plot $\log N$ against $1/T_{\max}$ to yield a value of Q . Doing this with the data of Ammann *et al.* [13] results in a value of $Q \approx 130 \text{ kcal mole}^{-1}$ which is less than the value found by experiment. In fact, because the role of n is ignored in this approach, the activation energy determined from the slope of the $\log N$ against $1/T_{\max}$ plot should be higher than the value of Q determined by actual measurement. It is the view of these writers that the total number (seven) of data points in the set of data of Ammann *et al.* [13] is too small to reliably establish the thermal fatigue behaviour of silicon nitride. Of the seven, four show significant data scatter for nearly identical values of T_{\max} , leaving only three data points to establish the effect of ΔT or T_{\max} on fatigue life. Three data points are not considered adequate in view of the statistical nature of brittle fracture of such materials as silicon nitride resulting from variations in crack size, geometry, orientation and other variables.

Such statistical effects were largely eliminated in the study of Hasselman *et al.* [20] on the thermal fatigue behaviour of circular rods of soda-lime-silica glass, thermally cycled from higher temperature into a water bath at a constant lower temperature. The excessive scatter in thermal fatigue data was reduced by promoting failure at artificial surface flaws introduced by diamond indentation. The data obtained and the property value for the glass can be used to numerically illustrate the relative influence of n and Q on thermal fatigue life.

For the soda-lime-silica glass rods investigated, $n \approx 16$ and $Q \approx 25 \text{ kcal mole}^{-1}$. In the fatigue experiments $T_{\max} \approx 433 \text{ K}$ and $\Delta T \approx 130^\circ \text{C}$. The relative change in thermal fatigue life which results from a decrease in T_{\max} and ΔT of 10°C will be calculated. Assuming that heat transfer occurred by forced convection as the result of the motion of the specimen through the water, substitution of the above values of n and Q in Equation 11 yields an increase in thermal fatigue life due to the decrease in ΔT by a factor of 3.6 whereas the decrease in T_{\max} increases thermal fatigue life by a

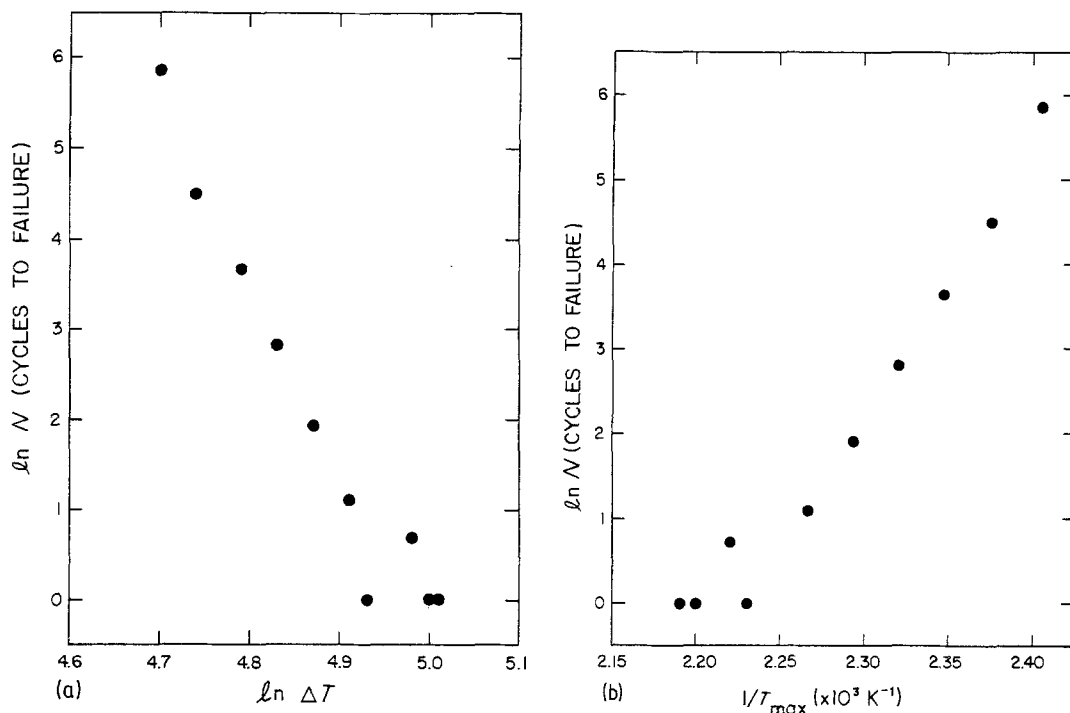


Figure 2 Thermal fatigue life of soda-lime-silica glass specimen subjected to repeated water quench (after [20]): (a) as a function of the initial temperature difference, (b) as a function of the maximum temperature.

factor approximately equal to 1.92. In the case of soda-lime-silica glass, then, the stress intensity exponent plays a more important role in establishing fatigue life than the activation energy. This contrasts with the previous findings for silicon nitride. Of course, such an effect is expected since for the silicon nitride the values of n and Q are lower and higher, respectively, than the corresponding values for the soda-lime-silica glass.

The data for the soda-lime-silica glass rods of Hasselman *et al.* [20] can be used to illustrate the erroneous values of n and Q , which can be obtained unless care is taken. Fig. 2a and b show the experimental data for the number-of-cycles to failure for the fifth specimen out of a total set of nine. Fig. 2a shows $\ln N$ plotted as a function of $\ln \Delta T$, whereas Fig. 2b shows the identical data plotted as a function of $1/T_{\max}$. Except for the data for 1 cycle-to-failure ($\log N = 0$), which may be governed by failure well before the end of the first cycle, both sets of data show reasonably linear behaviour. The slope of the data in Fig. 2a yields an apparent value for the stress intensity exponent of 22.7. This is significantly higher than the literature value [10] of n for this material, as expected since a plot of $\ln N$ against $\ln \Delta T$ does not reflect changes in the value of T_{\max} . Fig. 2b

results in an apparent value of $Q \approx 69 \text{ kcal mol}^{-1}$. This is far in excess of the experimental value, because a plot of $\ln N$ against $1/T_{\max}$ does not reflect the role of the stress intensity exponent in thermal fatigue life. Assuming the existence of natural convection during the thermal quench of the soda-lime-silica glass rods results in an only slightly lower value of n , because the value of the Biot number due to the thermal conductivity has a value near to 5 to 10.

Since the above numerical examples indicate that care needs to be exercised in the analysis of thermal fatigue data, the following recommendations are made: Values of thermal fatigue life should be established for two basic conditions; (1) T_{\max} should be kept constant with ΔT being varied by changing T_{\min} ; (2) ΔT should be kept constant by varying T_{\max} and T_{\min} by an equal amount. The data obtained for the first condition should result in an unambiguous value of n whereas the results for the second condition should give an unbiased value for Q . The data obtained in this manner should be sufficient to make predictions of thermal fatigue life for any combination of T_{\max} , T_{\min} and ΔT . If desired, additional experimental data can be obtained for verification of such predictions.

Equations 8 and 15 indicate that, even for identical specimen temperatures, the thermal fatigue life for natural and forced convection modes of heat transfer will be different. Therefore, for quantitative evaluation of thermal fatigue life, the mode of heat transfer must be established. Typically, in a thermal fatigue experiment, the hot specimen is inserted into a quenching bath at a lower temperature and held there for a specified period of time. Then, for a small specimen in a quenching medium (such as water) with a high heat transfer coefficient where the maximum stress could develop during the time period when the specimen is moving through the medium, the thermal fatigue life will be controlled by the forced convection mode of heat transfer. On the other hand, for a large specimen in a quenching medium (such as oil) with a low heat transfer coefficient where the maximum stress will develop during the hold period after insertion into the fluid, the fatigue life will be controlled by the natural convection. This suggests the need for *a priori* rough estimation of the mode of heat transfer before the quantitative data analysis can be made.

Some materials may show the existence of a pronounced fatigue limit, i.e. a value of stress intensity factor below which no slow crack growth occurs. This appears to be the case for polycrystalline mullite investigated by Kamiya and Kamigaito [15]. In case of such a pronounced fatigue limit, the expressions presented earlier will need to be modified. A further complexity in data analysis arises for heat transfer coefficients which may indicate a strong temperature dependence. For many fluid media, this can result from the effects of nucleate boiling and film formation. The corresponding changes in h with changes in T_{\max} , T_{\min} and ΔT could well play a major role in governing fatigue life. In particular, this could be the case with water, commonly used as a quenching medium. Extra caution is recommended in analysing data of thermal fatigue experiments obtained with water baths. For this reason, fluidized beds may be preferred over a water bath. However, in the use of a fluidized bed, caution must be exercised with specimens such as glass whose thermal fatigue life may be greatly influenced by surface conditions. The surface of a glass specimen may be damaged during its motion through the fluidized bed due to particle impact and the fatigue life may be greatly reduced. Therefore, the

effect of surface damage due to particle contact in the fluidized bed must be independently evaluated and incorporated in the quantitative evaluation and interpretation of the experimental data.

The above analyses also shed light on the effect of specimen size and material properties on thermal fatigue life. For high values of Biot number, Equations 8 and 15 indicate that thermal fatigue life is inversely proportional to the square of the dimensions of the specimen. On dimensional grounds, this conclusion should be generally valid regardless of geometry. For low values of Biot number, frequently encountered in laboratory studies and such components as silicon nitride and silicon carbide turbine blades and valves, a very pronounced size effect exists. For both forced and natural convection, Equations 8 and 15 suggest that

$$N \propto 1/R^{n+2} \quad \beta \ll 1. \quad (20)$$

This result indicates that major improvements in thermal fatigue life can be achieved by minor design changes in the form of even a slight reduction in component size.

In practice, the materials technologist may wish to select the material with highest thermal fatigue resistance. For a specimen of given size and geometry with a given crack size and configuration and given heat transfer environment, highest thermal fatigue resistance can be obtained by optimizing the relevant material properties which govern thermal fatigue failure. Materials with optimum thermal stress resistance can be selected on the basis of thermal stress resistance parameters or figures-of-merit which are available for a wide variety of heat transfer conditions and modes of thermal stress failure. Similar figures-of-merit can be defined for optimizing thermal fatigue resistance. For both forced and natural convection these can be obtained from Equations 8 and 15.

$$\frac{\kappa}{A(n-2)} \left[\frac{(1-\nu)k}{\alpha E} \right]^n \exp(Q/RT_{\max}) \quad \beta \ll 1 \quad (21a)$$

and

$$\frac{\kappa}{A(n-2)} \left[\frac{(1-\nu)k}{\alpha E} \right]^n \exp(Q/RT_{\max}) \quad \beta \gg 1. \quad (21b)$$

These figures-of-merit indicate that thermal fatigue life is governed by as many as seven material properties. Without quantitative infor-

mation on these properties, estimates of thermal fatigue life are not feasible. It is of interest to note that high thermal fatigue resistance requires high values of the thermal diffusivity κ , thermal conductivity, k , stress intensity factor exponent n and activation energy Q with low values of constant A , Young's modulus E and coefficient of thermal expansion α .

In this respect, for basic studies of thermal fatigue life, materials with low thermal diffusivity and conductivity may be most useful since thermal fatigue curves can be established with minimum number of cycles. Glassy materials, for this reason, appear most useful.

Acknowledgements

The present study was conducted as part of a research programme on the thermo-mechanical and thermo-physical properties of high-temperature structural materials supported by the Office of Naval Research under Contract: N00014-78-C-0431.

References

1. L. S. WILLIAMS, *Trans. Brit. Ceram. Soc.* **55** (1956) 287.
2. S. M. WIEDERHORN and L. H. BOLZ, *J. Amer. Ceram. Soc.* **53** (1970) 543.
3. J. E. RITTER, Jr and M. S. CAVANAGH, *ibid.* **59** (1976) 57.
4. J. E. RITTER Jr and C. L. SHEROURNE, *ibid.* **54** (1971) 601.
5. C. GURNEY and S. PEARSON, *Proc. Phys. Soc. London* **B62** (1958) 537.
6. RAM KOSSOWSKY, *J. Amer. Ceram. Soc.* **56** (1973) 531.
7. B. K. SARKAR and T. G. J. GLINN, *Trans. Brit. Ceram. Soc.* **69** (1970) 199.
8. V. I. TUMANOV, Z. A. GOLDBERG, V. V. CHERNYSHEV and A. I. PAVLOVA, *Poroshkovaya Metallurgiya* **10** (1966) 71.
9. R. C. BRADT, D. P. H. HASSELMAN and F. F. LANGE (Eds) "Fracture Mechanics of Ceramics, Vol. 2 Microstructure, Materials and Applications", (Plenum Press, New York, 1974).
10. A. G. EVANS, *J. Mater. Sci.* **7** (1972) 1137.
11. A. G. EVANS and E. R. FULLER, *Met. Tran.* **5** (1974) 27.
12. D. P. H. HASSELMAN, R. BADALIANCE, K. R. MCKINNEY and C. H. KIM, *J. Mater. Sci.* **11** (1976) 458.
13. C. L. AMMANN, J. E. DOHERTY and C. G. NESSLER, *Mater. Sci. Eng.* **22** (1976) 15.
14. D. P. H. HASSELMAN, E. P. CHEN, C. L. AMMANN, J. E. DOHERTY and C. G. NESSLER, *J. Amer. Ceram. Soc.* **58** (1973) 513.
15. N. KAMIYA and O. KAMIGAITO, *J. Mater. Sci.* **14** (1979) 573.
16. A. C. CHAPMAN, "Heat Transfer", 3rd edn (MacMillan Publishing Co., New York, 1967).
17. K. SATYAMURTHY, G. ZIEGLER, J. P. SINGH and D. P. H. HASSELMAN, unpublished work (1980).
18. J. C. JAEGER, *Philos. Mag.* **36** (1945) 418.
19. R. BADALIANCE, D. A. KROHN and D. P. H. HASSELMAN, *J. Amer. Ceram. Soc.* **57** (1974) 432.
20. D. P. H. HASSELMAN, E. P. CHEN and P. A. URICK, *Bull. Amer. Ceram. Soc.* **57** (1978) 190.
21. J. P. SINGH, J. R. THOMAS Jr and D. P. H. HASSELMAN, *J. Amer. Ceram. Soc.* **63** (1980) 140.

Received 11 February and accepted 26 March 1981.